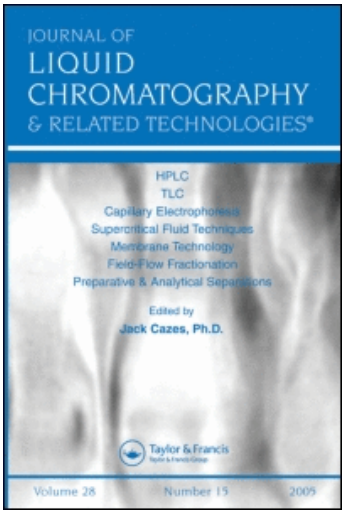

Journal of Liquid Chromatography & Related Technologies
Publication details, including instructions for authors and subscription information:
http://www.informaworld.com/smpp/title~content=t713597273

POTENTIAL-BARRIER FIELD-FLOW FRACTIONATION: POTENTIAL CURVES AND INTERACTIVE FORCES

George Karaiskakis[a]; Athanasia Koliadima[a]; Lambros Farmakis[a]; Dimitrios Gavril[a]
[a] Department of Chemistry, University of Patras, Patras, Greece

Online publication date: 28 August 2002

To cite this Article Karaiskakis, George , Koliadima, Athanasia , Farmakis, Lambros and Gavril, Dimitrios(2002) 'POTENTIAL-BARRIER FIELD-FLOW FRACTIONATION: POTENTIAL CURVES AND INTERACTIVE FORCES', Journal of Liquid Chromatography & Related Technologies, 25: 13, 2153 — 2172
To link to this Article: DOI: 10.1081/JLC-120013999
URL: http://dx.doi.org/10.1081/JLC-120013999

MARCEL DEKKER, INC. • 270 MADISON AVENUE • NEW YORK, NY 10016

JOURNAL OF LIQUID CHROMATOGRAPHY & RELATED TECHNOLOGIES
Vol. 25, Nos. 13–15, pp. 2153–2172, 2002

POTENTIAL-BARRIER FIELD-FLOW FRACTIONATION: POTENTIAL CURVES AND INTERACTIVE FORCES

George Karaiskakis,* Athanasia Koliadima, Lambros Farmakis and Dimitrios Gavril

Department of Chemistry, University of Patras,
GR-26504, Patras, Greece

ABSTRACT

Potential-barrier field-flow fractionation (PBFFF), a tool for the separation and size characterization of colloidal particles is based on the variation of the surface forces in the FFF process, which control particle adsorption–desorption on the channel wall. The latter phenomena depend on the total potential energy of interaction between the colloidal particles and the channel wall. Our results suggest, that at high ionic strengths of the suspending medium, the colloidal particles used (submicron monodisperse spherical particles of hematite and titanium dioxide) are retained within the secondary minimum even though the energy barrier is sufficiently high to inhibit attachment in the primary minimum of the interaction energy curve. This hypothesis is further supported by the particle detachment experiments at low ionic strengths of the suspension in which the total number of adhered particles was revealed when the secondary minimum

*Corresponding author. E-mail: g.karaiskakis@chemistry.upatras.gr

DOI: 10.1081/JLC-120013999
1082-6076 (Print); 1520-572X (Online)

MARCEL DEKKER, INC. • 270 MADISON AVENUE • NEW YORK, NY 10016

was eliminated. The secondary minimum energies, ϕ_{mn1}, necessary for the separation of the colloidal particles used in PBFFF, which were computed using the electrical double layers and van der Waals expressions were found, approximately, in the range $-4.7 < \phi_{mn1} < -3.2\,kT$, even though the energy maxima were much greater ($\phi_{max} \approx 10^9\,kT$). As the secondary minimum energies depend not only on the size of the particles, but also on their nature, one could separate by PBFFF particles of different size, as well as of the same size but with different chemical constitution.

Key Words: Potential curves; Interactive forces; Field-flow fractionation; Potential-barrier field-flow fractionation

INTRODUCTION

The nature and strength of the adhesive bonds holding microscopic particles on flat surfaces, and the related resistance to external forces which tend to break these bonds, are directly related to strength and structure of aggregates, to breakage processes in crystallization, to chromatographic separations, to colloid-facilitated transport of pollutants in soils, and groundwater aquifers,[1–6] etc. Furthermore, adhesion plays an important role in fraction behaviour of surfaces, as well as in particulate collisions in order to investigate the role of colloidal and hydrodynamic forces in particle–particle and particle–surface interaction phenomena.[5,6] The adhesion and detachment of colloidal particles from a flat solid surface were also the main processes in Potential-Barrier Field-Flow Fractionation (PBFFF).[7–14] In PBFFF no chemical bonding is involved which would cause irreversible binding of the particles, but only forces of a physicochemical nature.

Potential-barrier field-flow fractionation can be applied to separate particles based on differences in size and/or in any of the physicochemical parameters involved in the potential energy of interaction between the particles and the channel wall. In its simplest form, the technique consists in changing the ionic strength of the suspending medium from a high value, where only one of the colloidal materials of the mixture with the lower attractive force with the channel wall is eluted out from the channel, while the rest ones are totally adhered at the beginning of the SdFFF wall. Then, a programmed decrease of the ionic strength of the carrier solution is applied to release, in time, the adherent particles according to their size and/or surface characteristics. The method has been successfully applied to the size fractionation and characterization of monodisperse submicron particles of hematite and titanium dioxide,[7–9,12] of

monodisperse submicron particles of polymethylmethacrylate (PMMA),[13] and of various supramicron polydisperse irregular particles of mixed sulfides.[10,11] The same technique was also used for the concentration and size characterization of dilute colloidal samples, in both the normal and the steric modes of operation in sedimentation FFF.[9,14]

The purpose of the present paper is to reexamine the role of colloidal forces in PBFFF, so as to understand better the potential mechanisms governing adhesion and conditions under which release of deposited particles may occur. The work focuses on the effects of secondary minima caused by the combined action of weak double-layer repulsion and van der Waals attraction on deposition and the potential release of colloids in PBFFF due to changes in the suspension's ionic strength.

EXPERIMENTAL

Materials

Hematite nearly monodisperse spherical particles of two sizes [a-Fe_2O_3(I) with $d = 0.146\,\mu m$ and a-Fe_2O_3(II) with $d = 0.258\,\mu m$], supplied by Prof. J. Lyklema (Agricultural University, Wageningen, The Netherlands), and titanium dioxide monodisperse spherical particles from Polysciences, Inc. with $d = 0.310\,\mu m$ were used as model samples.

The suspending medium was triply distilled water containing 0.5% (v/v) of detergent FL-70 and 0.02% (w/w) sodium azide as bacteriocide. The electrolyte added to this carrier solution in order to adjust its ionic strength was potassium nitrate (KNO_3) from Riedel-de Haën.

Apparatus and Procedure

The basic sedimentation FFF (SdFFF) system used in this study for testing the PBFFF procedure has been described in detail elsewhere.[7–9] The dimensions of the SdFFF system were $38.4\,cm \times 2.35\,cm \times 0.0197\,cm$ with a channel void volume of $1.68\,cm^3$, measured by the elution of the non-retained peak of sodium benzoate. The outside wall of the channel, which was placed 6.85 cm from the center of rotation, was bare polished Hastelloy C alloy, which is principally Ni (56%) with 17% Mo, 15% Cr, 5% Fe, 4% W, and traces of Mn and Si.[15] As the Hastelloy C material is one of the most generally corrosion-resistant alloys commercially available, and we don't know its surface potential, we will use in all of our calculations in the "Results and Discussion" section, as surface potential of the Hastelloy C, that of stainless steel given in the literature.[16,17]

Detection in the SdFFF system was accomplished by means of a Gilson model 111 Holochrome UV detector (operating at 254 nm), while a Gilson Minipuls peristaltic pump was used to pump the carrier solution and the samples into the channel.

The electrophoretic mobilities of the colloidal particles used in the present work, were measured in a microelectrophoresis apparatus (Rank, Mark II) by using a four-electrode capillary cell. The velocities of at least twenty particles in each direction of the electric field were measured at the two stationary layers with an accuracy of ±10%. The pH of the colloidal suspensions was measured by using a combination glass-saturated calomel electrode (Metrohm), and was kept constant (pH = 9.5) in all cases. All experiments were performed at 25°C.

RESULTS AND DISCUSSION

The separation of the monodisperse spherical particles of a-Fe_2O_3(I), with diameter $d = 0.146\,\mu m$, from those of the same material (a-Fe_2O_3(II)) but with different diameter $d = 0.258\,\mu m$, can be achieved easily by conventional SdFFF (cf. Fig. 1a), as the corresponding retention volumes, V_R, are proportional to the cube of the diameter:[7,14]

$$V_R = V_o\left(\frac{\pi d^3 G w \Delta\rho}{36kT}\right) \quad (1)$$

where V_o is the column void volume, G is the sedimentation field strength expressed in acceleration, w is the channel thickness, $\Delta\rho$ is the density difference between the particle and the medium, k is Boltzmann's constant and T is the absolute temperature.

The difference in the V_R values, ΔV_R, corresponding to the two samples, as they were calculated from Eq. (1) is 27.6 cm^3, a value which is into the limits of the critical resolution in conventional SdFFF, so as to assure complete separation of the a-Fe_2O_3(I) and a-Fe_2O_3(II) particle. A similar separation by the conventional SdFFF technique, which is based not only on the size's difference but also on the $\Delta\rho$ difference, is presented in Fig. 2a for the samples of a-Fe_2O_3(I) and TiO_2. In both cases (cf. Figs. 1a and 2a), the fractionation is based principally on size differences, even in the second case the resolution is also dependent on the difference of the density differences.

Of particular interest is the separation not only of particles with different size, but also of particles with the same size, which have different chemical nature by the PBFFF technique. Potential-barrier field-flow fractionation can be applied to separate particles based on differences in size or in any of the physicochemical parameters involved in the potential energy of interaction between the particles

MARCEL DEKKER, INC. • 270 MADISON AVENUE • NEW YORK, NY 10016

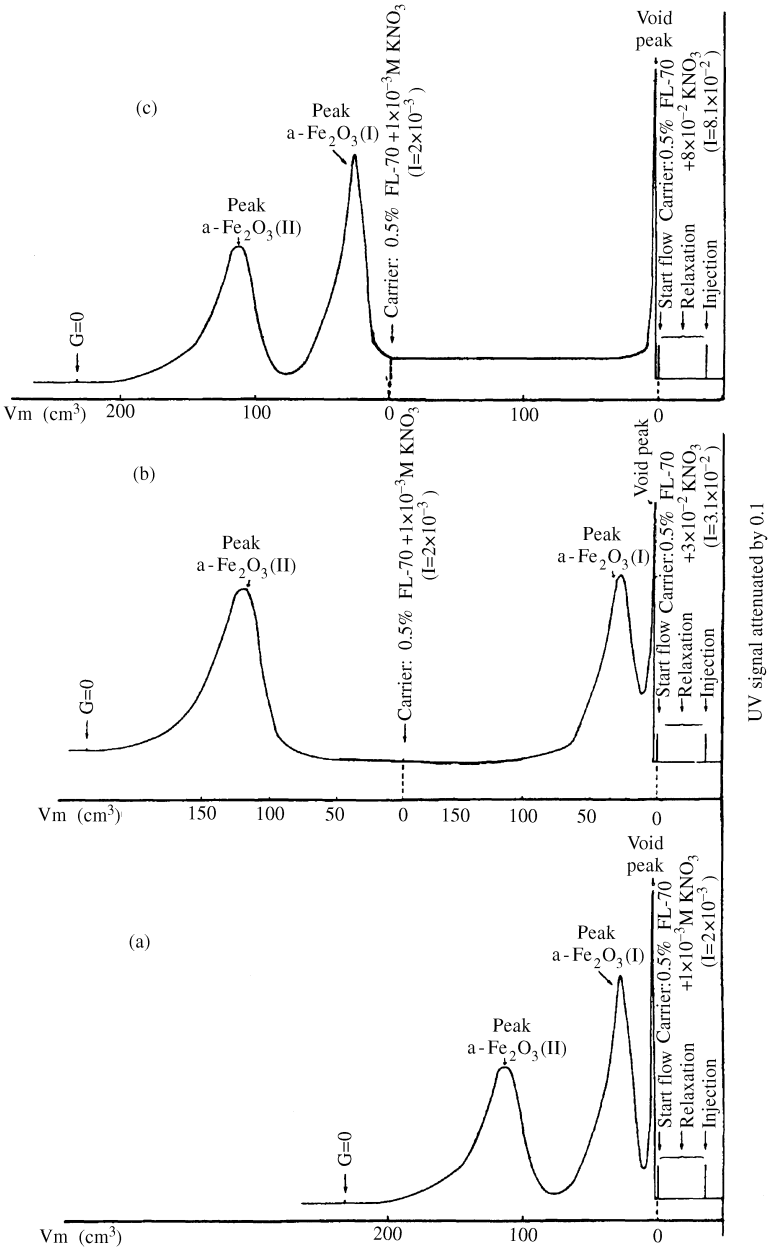

Figure 1. Fractionation of a-Fe_2O_3(I) and a-Fe_2O_3(II) particles by conventional SdFFF (a) and (c) and by PBFFF (b).

MARCEL DEKKER, INC. • 270 MADISON AVENUE • NEW YORK, NY 10016

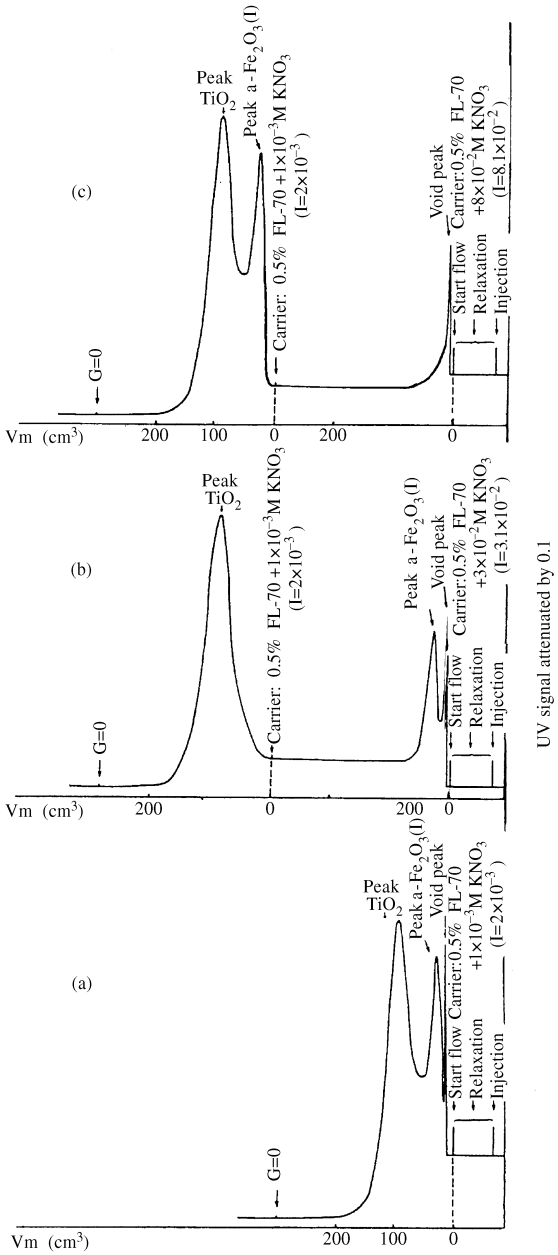

Figure 2. Fractionation of a-Fe_2O_3(I) and TiO_2 particles by conventional SdFFF (a) and (c) and by PBFFF (b).

and the channel wall.[7–14] Even the used colloidal particles should be fractionated by the conventional SdFFF technique; it is preferable to be separated by the PBFFF, as its resolution is much higher than the previous one.

The fractionation of a-Fe_2O_3(I) and a-Fe_2O_3(II) particles, as well as of a-Fe_2O_3(I) and TiO_2 particles by PBFFF is presented in Figs. 1b and 2b. When the ionic strength is 3.1×10^{-2}, the a-Fe_2O_3(II) particles in Fig. 1b and the TiO_2 particles in Fig. 2b are adhered at the beginning of the SdFFF channel wall, even though the a-Fe_2O_3(I) particles in both cases are eluted out from the column. A further increase of the suspension ionic strength (8.1×10^{-2}) leads also to the total adhesion of the a-Fe_2O_3(I) (cf. Figs. 1c and 2c). Variation of the carrier solution to one containing a lower ionic strength (2×10^{-3}) released all of the adherent a-Fe_2O_3(I) and a-Fe_2O_3(II) particles (cf. Fig. 1c), as well as of the a-Fe_2O_3(I) and TiO_2 particles (cf. Fig. 2c). The differences in the V_R values between the conventional SdFFF and the PBFFF are very close, indicating that PBFFF can be applied not only for the fractionation of particles but also for their accurate size determination.

The total potential energy of interaction between a spherical particle and a solid surface in a dispersing medium, ϕ, is the sum of the van der Waals attraction energy, ϕ_A, and the electric double layer potential repulsion, ϕ_R, which in reduced form, in kT units (as kT is the thermal energy), can be written in the form:[8,17–19]

$$\phi = \phi_A + \phi_R = -\frac{A_{132}}{6kT}\left[\ln\left(\frac{h+d}{h}\right) - \frac{2a(h+a)}{h(h+d)}\right] + \frac{16\varepsilon\varepsilon_0 a}{kT}\left(\frac{kT}{e}\right)^2 \times \tanh\left(\frac{e\psi_p}{4kT}\right)\tanh\left(\frac{e\psi_w}{4kT}\right)e^{-h/\lambda} \quad (2)$$

where A_{132} is the effective Hamaker constant for media 1 (particle) and 2 (channel wall) interacting across medium 3, h is the separation distance between the particle nearest surface and the channel wall, α is the particle radius, ε is the dielectric constant, e_0 is the permitivity of the vacuum, ε_0 is the charge of an electron, ψ_p and ψ_w are the surface potentials of the particle and the wall, respectively, and λ is the Debye length, which for aqueous media at 25°C, is computed from the relation:

$$\lambda = 0.304I^{-1/2} \quad (3)$$

where I is the medium's ionic strength.

Equation (2) shows that for a given system (particle–wall) the interaction energy between the particles and the wall depends mainly on the effective Hamaker constant, the surface potentials of the particles and the wall and the ionic strength of the suspension.

In all experiments of the present work, the adhesion–detachment processes, which control the separation by PBFFF were achieved by the variation of the ionic strength, and consequently, by the variation of the Debye's length. The critical ionic strengths of the dispersing medium, so as the whole number of the particles to be adhered at the beginning of the SdFFF channel wall, as well as those for their total release with the corresponding Debye's lengths, are compiled in Table 1. In all cases, the adhesion Debye's length is much smaller than the detachment one. Furthermore, there is a critical value of the Debye length where the profile of the potential of the particle–wall interaction changes form, and the particles are totally adhered at the SdFFF channel wall. As the Debye length is immediately related to the closest distance of separation of the particles from the substrate, h, we will calculate the total potential energy of interaction ϕ, as a function of the distance h, at various ionic strengths of the suspending medium for all the samples used in the present work.

For the calculation of ϕ with the aid of Eq. (2), we will use the values of the necessary quantities from various sources, which are summarized in Table 2. As pointed out by Hogg et al.[20] it seems reasonable to assume that the Hamaker constant is approximately the same for inorganic oxides dispersed in an aqueous medium, since the surfaces are essentially similar, being composed primarily of oxygen anions. The value of A_{132} for the systems steel–water–inorganic oxides [a-Fe_2O_3(I), a-Fe_2O_3(II) and TiO_2] was supposed to be kept constant in all cases, as the Hamaker constants are practically independent on the suspension pH and ionic strength, and so may be considered as fixed in a first approximation. The A_{132} value was calculated from the Hamaker constants of stainless steel (A_{11}), inorganic oxides (A_{22}), and water (A_{33}) by using the Eq. (8) of Ref. 8.

Even the ionic strength generally influences the zeta-potentials, and consequently, the surface potentials of the particles and the SdFFF channel wall.

Table 1. Debye's Lengths for the Adhesion ($\lambda^{adh.}$) and Detachment ($\lambda^{det.}$) of the Particles as a Function of the Corresponding Ionic Strengths $I^{adh.}$ and $I^{det.}$ of the Suspending Medium

Sample	d (μm)	$I^{adh.}$	$I^{det.}$	$\lambda^{adh.}$ (nm)	$\lambda^{det.}$ (nm)
a-Fe_2O_3(I)	0.146	8.1×10^{-2}	—	1.08	—
		—	2.0×10^{-3}	—	6.87
a-Fe_2O_3(II)	0.258	3.1×10^{-2}	—	1.74	—
		—	2.0×10^{-3}	—	6.87
TiO_2	0.310	3.1×10^{-2}	—	1.74	—
		—	2.0×10^{-3}	—	6.87

Table 2. Collection of Parameters Used in the Calculation of Particle–Wall Interaction Energies in PBFFF

Material	Hamaker Constant ($10^{20} \times A/J$)	Surface Potential (mV)	Literature
a-Fe_2O_3(I)	$A_{22} = 6.2$	−15.6	8, 16
a-Fe_2O_3(II)	$A_{22} = 6.2$	−15.6	8, 16
TiO_2	$A_{22} = 6.2$	−45.7	8, 16
H_2O	$A_{33} = 4.4$	—	8, 16
Stainless steel (SS)	$A_{11} = 22.0$	−24.0	8, 16, 17
SS–H_2O–I.O.*	$A_{132} = 1.02$	—	8, 16

*I.O. = Inorganic Oxide [a-Fe_2O_3(I), a-Fe_2O_3(II), TiO_2].

Previous works[17,21] have shown that the variation of the ionic strength to such extent as used in the present work, doesn't change, significantly, the surface potentials both of the particles and of the wall. It can be attributed, among other reasons, to the fact that the suspension pH was kept constant (pH = 9.5) in all cases. The latter indicates that the used variation of the electrolyte concentration, so as the interaction forces between the particles and the wall in PBFFF to be converted from repulsive to attractive ones and vice-versa, influences, mainly, the exponential factor of the repulsive portion of ϕ in Eq. (2), through the variation of the Debye's length and/or the nearest distance between the particle and the substrate. It must also be pointed out that the zeta-potentials of the particles (as they were measured by the microelectrophoresis apparatus) and the substrate (as was found in Ref. 17) have both negative values at the working pH = 9.5, indicating a situation unfavorable for the deposition of particles on the substrate. This can be overcome by using sufficiently high ionic strength suitable to compress the double layer, and consequently, to eliminate the electrostatic repulsion.

The variation of the total potential energy of interaction between the particles and the SdFFF channel wall, as a function of their separation distance, is presented in Figs. 3–5. In all cases, an enormous potential barrier very close to the substrate appeared, whose height is independent of the ionic strength of the suspending medium. As the adhesion and detachment processes, which control the separation of particles in PBFFF, are strongly dependent on the suspension's ionic strength, it is obvious that the adsorption and desorption of particles in PBFFF doesn't take place at the potential barrier, but within the secondary minimum whose depth is strongly dependent on the medium's ionic strength (cf. Figs. 3–5).

A better and more distinct picture of the total potential energy of interaction between the particles and the SdFFF channel, at the conditions of their adhesion and detachment for which we are more interested in PBFFF, as a function of the separation distance, is presented in Figs. 6–8. All these figures show that while the

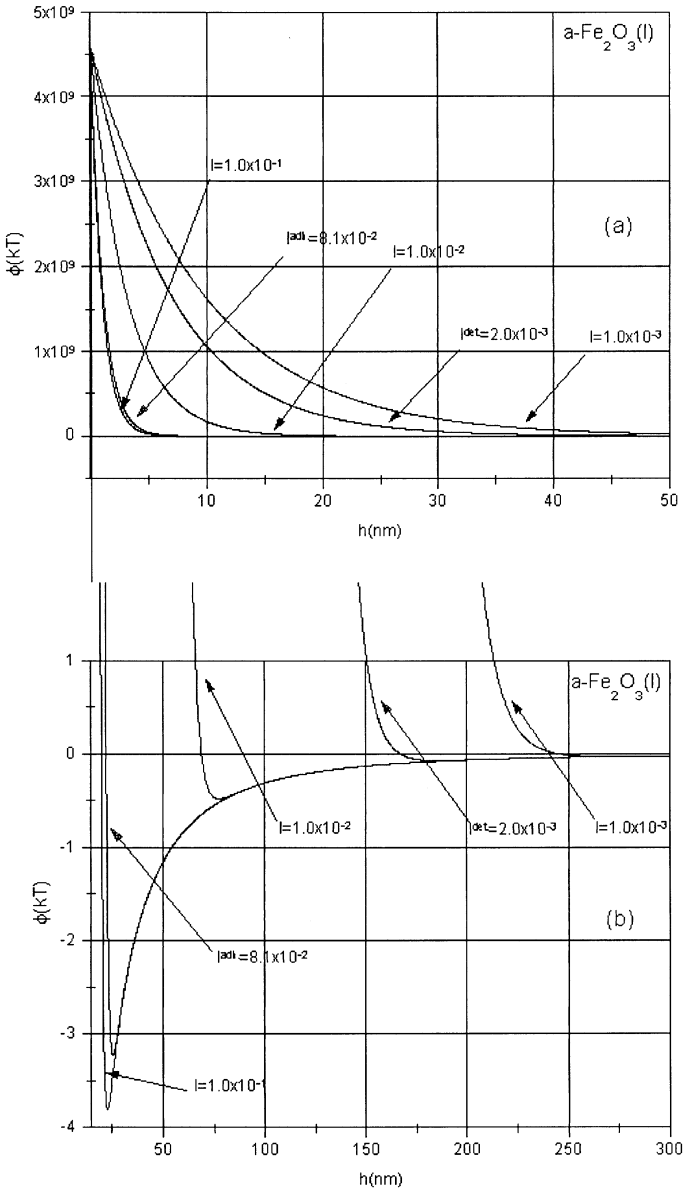

Figure 3. Total potential energy of interaction, ϕ, between the a-Fe_2O_3(I) particles and the SdFFF channel wall as a function of the distance, h, between the particles and the substrate at various ionic strengths, I, of the suspending medium showing the potential barrier (a) and the secondary minimum (b).

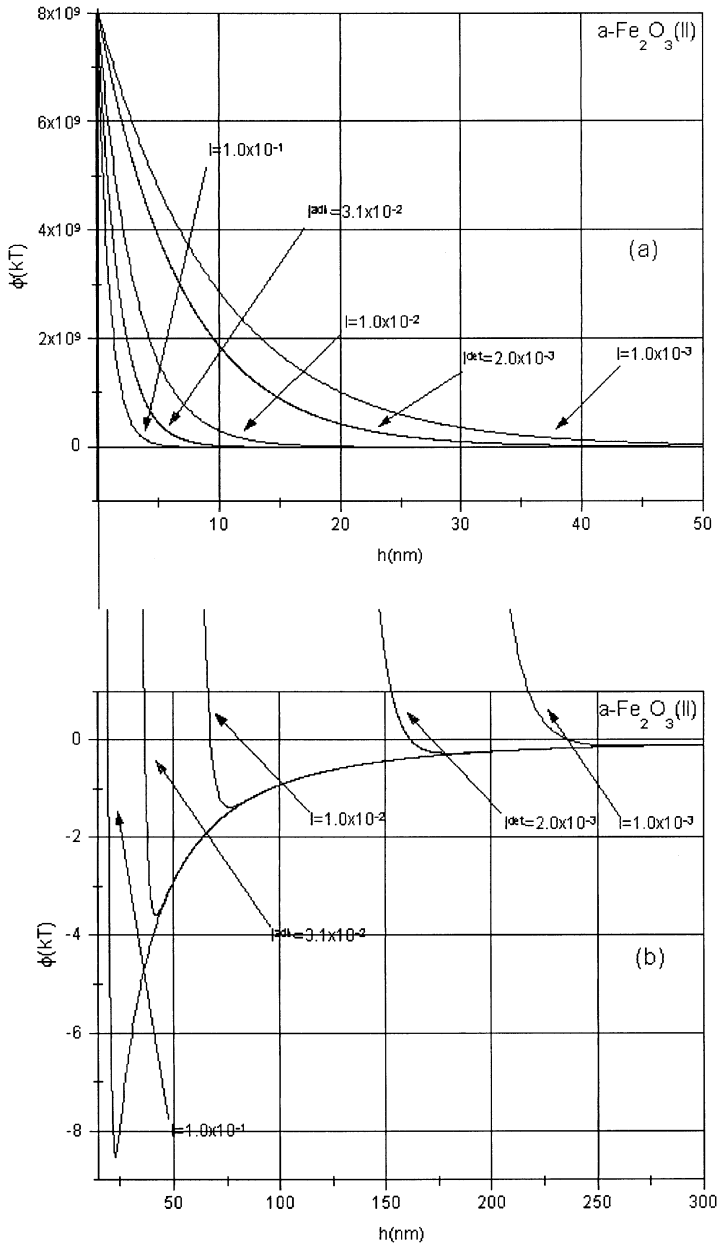

Figure 4. Variation of ϕ with h for the a-Fe_2O_3(II) particles at various ionic strengths of the suspending medium showing the potential barrier (a) and the secondary minimum (b).

MARCEL DEKKER, INC. • 270 MADISON AVENUE • NEW YORK, NY 10016

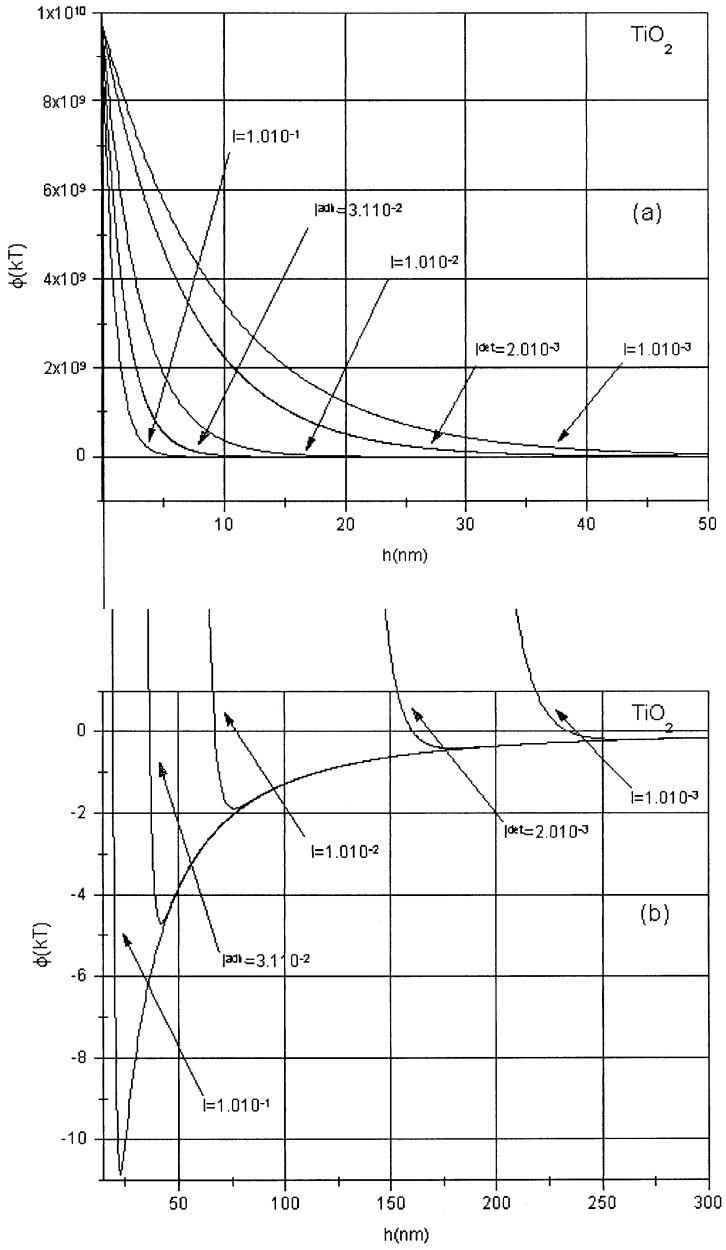

Figure 5. Variation of ϕ with h for the TiO_2 particles at various ionic strengths of the suspending medium showing the potential barrier (a) and the secondary minimum (b).

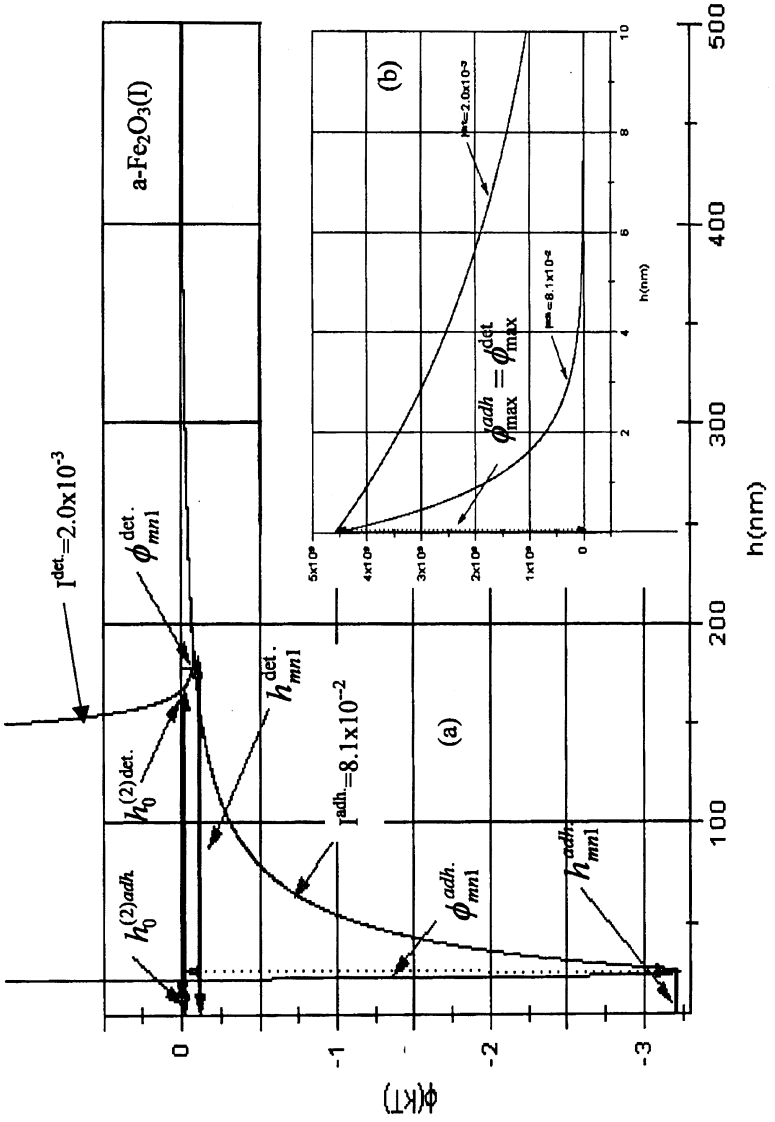

Figure 6. Total potential energy of interaction between the a-Fe_2O_3(I) and the substrate as a function of the distance h at conditions of adhesion and detachment showing the secondary minimum (a) and the potential barrier (b).

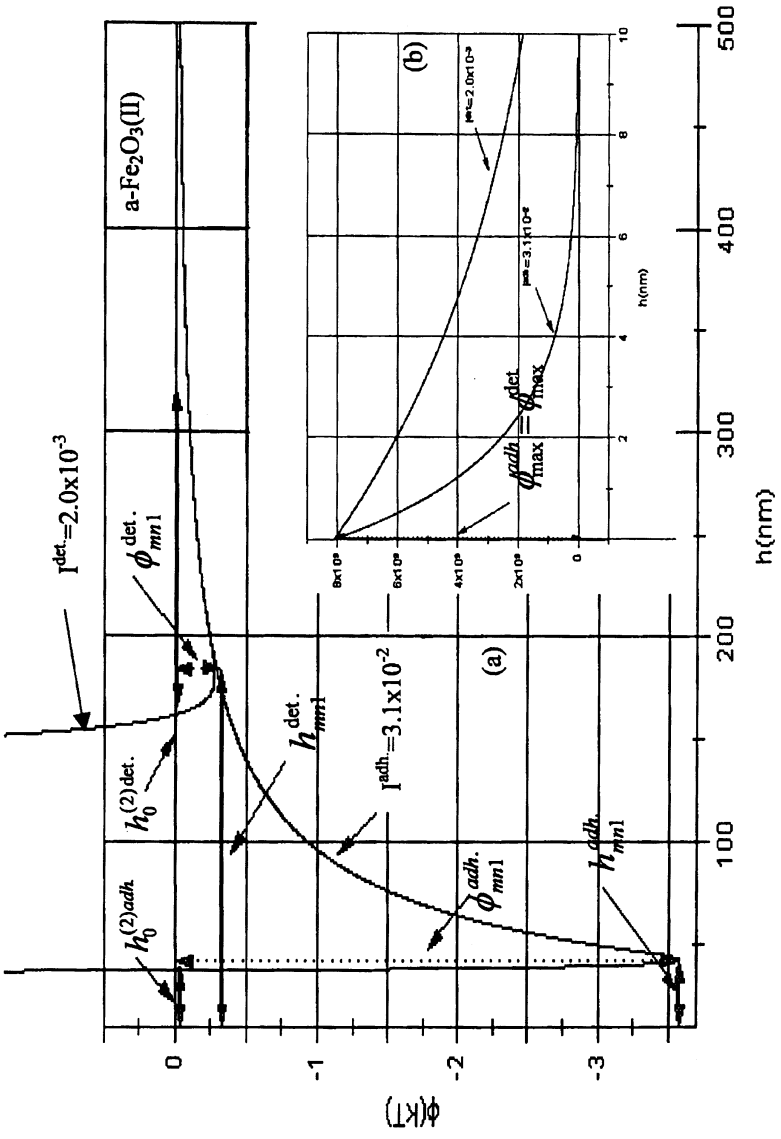

Figure 7. Dependence of ϕ on h for the adhesion and detachment of a-Fe_2O_3(II) particles showing the secondary minimum (a) and the potential barrier (b).

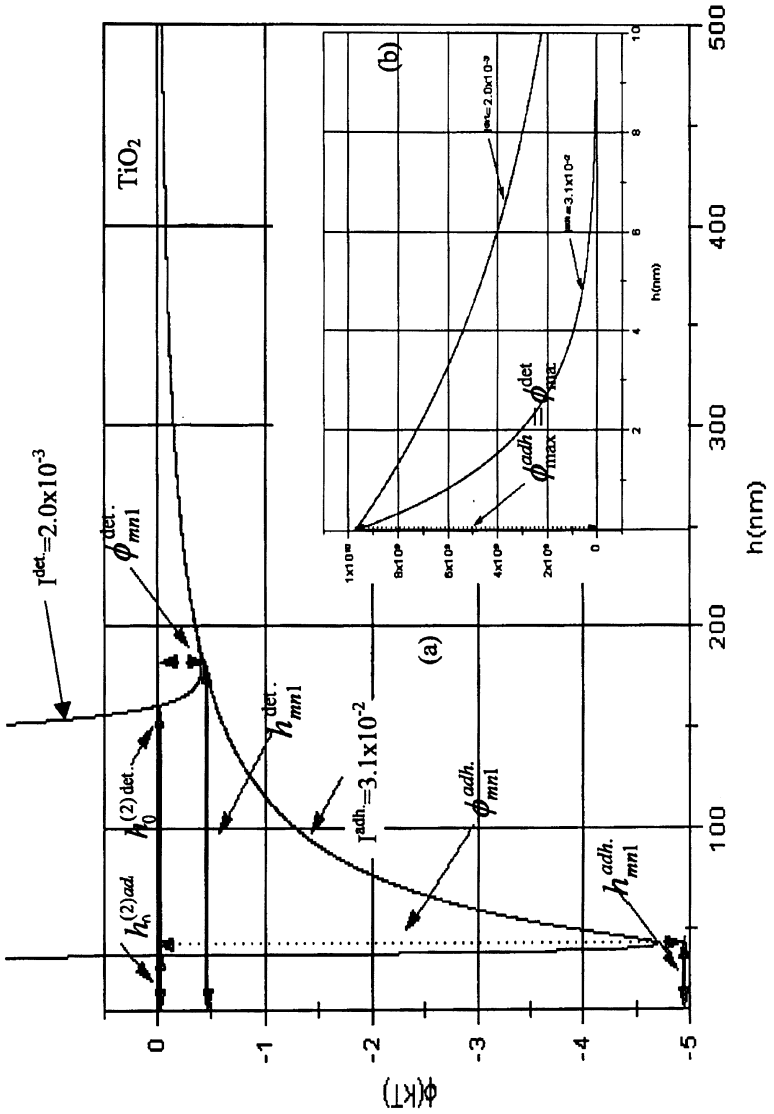

Figure 8. Variation of ϕ with h for the conditions of adhesion and detachment of the TiO_2 particles showing the secondary minimum (a) and the potential barrier (b).

potential barrier is enormous and its magnitude is approximately the same for the adhesion and detachment processes, the depth of the secondary minimum, which is dependent on the size and the nature of the particles, for the conditions of adhesion lies in the range $-4.70 < \phi_{mn1}^{adh.} < -3.23\,kT$, while for those of detachment is very close to zero ($-0.40 < \phi_{mn1}^{det.} < -0.08\,kT$). The values of $\phi_{max}^{2adh.}$, $\phi_{max}^{det.}$, $\phi_{mn1}^{adh.}$ and $\phi_{mn1}^{det.}$, as well as the separation distances, which correspond to the energy barrier ($h_{max}^{adh.}$ and $h_{max}^{det.}$), to the secondary minimum ($h_{mn1}^{adh.}$ and $h_{mn1}^{det.}$), and to the first and second zero potential energy of interaction ($h_0^{(1)adh.}$, $h_0^{(1)det.}$, $h_0^{(2)adh.}$ and $h_0^{det.}$) are presented in Tables 3–6. As the distance corresponding to the first zero energy, $h_0^{(1)}$, we mean the location of the first zero in the potential energy curve, which appears between the primary minimum and the barrier, while as the distance corresponding to the second zero energy, $h_0^{(2)}$, the location of the second zero, which appears between the maximum and the secondary minimum.

From the Figs. 6–8 and the Tables 3–6 the following conclusions can be drawn:

1. The height of the barrier is enormous ($\sim 10^9\,kT$), but independent of the ionic strength, as is the same for both the conditions of adhesion and detachment. It is also dependent on the size and the chemical nature of the colloidal particles.

2. The deep of the secondary minimum is dependent on the suspension's ionic strength, as it is different for the conditions under which adhesion and detachment take place. The secondary minimum of the interaction profile becomes more prominent as the ionic strength and particle size increases. Thus, particle adhesion in the secondary minimum explains their reversible adsorption in PBFFF, even though the energy barrier is sufficient to prevent attachment in the primary minimum of the interaction energy curve. The physical interpretation of particle escape, at conditions of detachment at which the secondary minimum approaches zero, over a sharp maximum, is that the particles have such a short distance to travel ($h_{max}^{det.} \approx 10^{-4}$ nm, cf. Table 5), in order to be free of the substrate (e.g., to be detached from the SdFFF channel wall), that friction has a negligible role in impeding their detachment. As noted above, the depth of the

Table 3. Maximum, ϕ_{max}, and Secondary Minimum, ϕ_{mn1}, Energies for the Adhesion and Detachment of the Particles Used on and from the SdFFF Channel Wall

		Adhesion		Detachment	
Sample	d (μm)	$\phi_{max}\,(kT)$	$\phi_{mn1}\,(kT)$	$\phi_{max}\,(kT)$	$\phi_{mn1}\,(kT)$
a-Fe_2O_3(I)	0.146	4.58×10^9	−3.23	4.58×10^9	−0.08
a-Fe_2O_3(II)	0.258	8.09×10^9	−3.58	8.09×10^9	−0.28
TiO_2	0.310	9.72×10^9	−4.70	9.72×10^9	−0.40

Table 4. Separation Distances, h_{mn1}, Corresponding to the Secondary Minimum for the Adhesion and Detachment of the Used Particles, as Well as Effective Thicknesses of the Excluded Regions, $h_{eff}(=h_{mn1}+d/2)$

		h_{mn1} (nm)		$h_{eff.}$ (nm)	
Sample	d (μm)	Adhesion	Detachment	Adhesion	Detachment
a-Fe_2O_3(I)	0.146	25	185	98	258
a-Fe_2O_3(II)	0.258	42	181	171	310
TiO_2	0.310	42	180	197	335

secondary minimum is comparable to kT at high ionic strengths. Of course, the location and magnitude of this minimum also depends on the Hamaker constants and the surface potentials of the particles and the wall. Since the depth depends on the particle's chemical nature at high ionic strengths, we could separate, by PBFFF, particles of the same size, which have a different chemical constitution. It is also interesting to note, that greatest selectivity among different sizes of particles of the same chemical species can be obtained at high ionic strengths.

3. The separation distances, which correspond to the adhesion within the secondary minimum, are smaller than those corresponding to detachment. The latter distances approximate the values of the relative particle diameters. Generally speaking, the secondary minimum appears at relatively long distances, compared to those corresponding to the primary minimum and to the energy barrier, at which attractive forces dominate over the repulsion, even for a stable colloid. By adding to the separation distance h_{mn1} the radius of the particle, we obtain the effective thickness of the excluded region, which increases as the ionic strength decreases.

Table 5. Separation Distances, h_{max}, Corresponding to the Energy Barrier for the Adhesion and Detachment of the Colloids on and from the SdFFF Channel Wall

		$10^4 \times h_{max}$ (nm)	
Sample	d (μm)	Adhesion	Detachment
a-Fe_2O_3(I)	0.146	2.05	5.18
a-Fe_2O_3(II)	0.258	2.62	5.18
TiO_2	0.310	2.61	5.18

Table 6. Separation Distances Corresponding to the First* ($h_0^{(1)}$) and the Second** ($h_0^{(2)}$) Zero Potential Energy of Interaction Between the Colloids and the SdFFF Channel Wall at Conditions of Adhesion and Detachment

		$10^8 \times h_0^{(1)}$ (nm)		$h_0^{(2)}$ (nm)	
Sample	d (μm)	Adhesion	Detachment	Adhesion	Detachment
a-Fe_2O_3(I)	0.146	4.00	4.00	22	167
a-Fe_2O_3(II)	0.258	3.95	3.95	37	162
TiO_2	0.310	3.95	3.95	37	161

*The zero in the potential energy curve before the maximum barrier.
**The zero between the maximum and the secondary minimum.

4. The separation distances, which correspond to the energy barrier, and to the first zero energy, which appears between the primary minimum and the energy barrier, are extremely low ($\sim 10^{-4}$ nm), indicating that adsorption of particles within the primary minimum is not possible. In support of the above assumption, is the fact that reversible attractive forces at the particle–wall interface in PBFFF may be associated with deposition in a secondary minimum. The separation distances, which correspond to the second zero energy appearing between the maximum and the secondary minimum, are in the order of particle size and very close to the separation distances corresponding to the secondary minimum. All these separation distances are strongly dependent on the ionic strength of the suspending medium, making possible the alteration of the total potential energy of interaction between the particles and the SdFFF channel wall in PBFFF to such extent, so as the adhesion conditions could be easily converted to the detachment ones, or vice-versa, by suitable variation of the suspension's ionic strength.

CONCLUSIONS

The presence of the "secondary" potential energy minimum, at which the attractive forces dominate over the repulsion when the ionic strength is high enough to assure total adhesion of the colloids at the beginning of the SdFFF channel wall, shows that this secondary minimum is responsible for the reversible adsorption–desorption phenomena in PBFFF.

On the other hand, the almost absence of this secondary minimum when the suspension's ionic strength is too low to assure total detachment of the adhered particles, supports our hypothesis that it is the secondary minimum which controls the resolution in PBFFF, and not the energy barrier, as its height is

enormous and independent of the ionic strength. The total release of the adhered particles, as it is verified either by the surface area of the eluted peaks in conventional and PBFFF techniques or by the observation that no elution peak was obtained even when the field strength was reduced to zero, supports our previous conclusion that the reversible adhesion–detachment of particles in PBFFF takes place within the secondary minimum.

As a general conclusion, at high ionic strengths of the suspending medium, the diffused part of the electric double layer is compressed and the thickness of the ionic atmosphere diminishes. At the same time, the compression of the ionic layer deepens the secondary minimum, thus making further adhesion more probable. On the other hand, at low ionic strengths, the extension of the ionic layer disappears from the secondary minimum, thus making possible the particle's detachment.

ACKNOWLEDGMENT

The authors thank Mrs. M. Barkoula for her kind assistance.

REFERENCES

1. Ryan, J.N.; Gschwend, P.M. J. Colloid Interface Sci. **1994**, *164*, 21–34.
2. Ryde, N.; Matijevic, E. J. Colloid Interface Sci. **1995**, *169*, 468–475.
3. Nocito-Gobel, J.; Tobiason, J.E. Colloids Surfaces A **1996**, *107*, 223–231.
4. Haber, S.; Brenner, H. J. Colloid Interface Sci. **1993**, *155*, 226–246.
5. Elimelech, M. J. Colloid Interface Sci. **1994**, *164*, 190–199.
6. Yiantsios, S.G.; Karabelas, A.J. J. Colloid Interface Sci. **1995**, *176*, 74–85.
7. Karaiskakis, G.; Koliadima, A. Chromatographia **1989**, *28*, 31–32.
8. Koliadima, A.; Karaiskakis, G. J. Chromatogr. **1990**, *517*, 345–359.
9. Koliadima, A.; Karaiskakis, G. Chromatographia **1994**, *39*, 74–78.
10. Athanasopoulou, A.; Karaiskakis, G. Chromatographia **1995**, *40*, 734–736.
11. Athanasopoulou, A.; Karaiskakis, G. Chromatographia **1996**, *43*, 369–372.
12. Karaiskakis, G.; Athanasopoulou, A.; Koliadima, A. J. Microcol. Sep. **1997**, *9* (4), 275–280.
13. Karaiskakis, G.; Douma, M.; Katsipou, I.; Koliadima, A.; Farmakis, L. J. Liq. Chromatogr. & Rel. Technol. **2000**, *23*, 1953–1959.
14. Karaiskakis, G. In *Encyclopedia of Chromatography*; Cazes, J., Ed.; Marcel Dekker, Inc.: New York, 2001; 653–656.
15. Fontana, M.G.; Greene, N.D. *Corrosion Engineering*; Mc-Graw-Hill Co.: New York, 1978; 175.
16. Kuo, R.J.; Matijevic, E. J. Colloid Interface Sci. **1980**, *78*, 407–420.

17. Hansen, M.E.; Giddings, J.C. Anal. Chem. **1989**, *61*, 811–819.
18. Hiemenz, P.C. *Principles of Colloid and Surface Chemistry*; Marcel Dekker, Inc.: New York, 1977; 457–467.
19. Prieve, D.C.; Hoysan, P.M. J. Colloid Interface Sci. **1978**, *64*, 201–213.
20. Hogg, R.; Healy, T.W.; Fuerstenau, D.W. Trans. Faraday Soc. **1966**, *62*, 1638–1651.
21. Litton, G.M.; Olson, T.M. Colloids Surfaces A **1996**, *107*, 273–283.

Received March 22, 2002
Accepted April 29, 2002
Manuscript 5819